

# Sonographic Dynamic Description of the Laryngeal Tract

## Definition of Quantitative Measures to Characterize Vocal Fold Motion and Estimation of Their Normal Values

Héloïse Bergeret-Cassagne, MD, Diane S. Lazard, MD, Muriel Lefort, BSc, Siham Hachi, MSc, Laurence Leenhardt, MD, PhD, Fabrice Menegaux, MD, PhD, Gilles Russ, MD, Christophe Trésallet, MD, PhD, Frédérique Frouin, PhD

Received on May 9, 2016, from the Sorbonne Universités, UPMC Univ Paris 06, AP-HP, Hôpital Pitié-Salpêtrière, Department of General, Visceral and Endocrine Surgery, Paris, France (H.B.-C., D.S.L., F.M., C.T.); Sorbonne Universités, UPMC Univ Paris 06, CNRS, Inserm, Laboratoire d'Imagerie Biomédicale (LIB), Paris, France (H.B.-C., M.L., S.H., L.L., C.T.); Institut Arthur Vernes, ENT Surgery, Paris, France (D.S.L.); Sorbonne Universités, UPMC Univ Paris 06, AP-HP, Hôpital Pitié-Salpêtrière, Thyroid and Endocrine Tumors Department, Paris, France (L.L., G.R.); and Inserm, CEA, Univ Paris-Sud, CNRS, Université Paris-Saclay, Laboratoire Imagerie Moléculaire In Vivo (IMIV), CEA/I2BM/Service Hospitalier Frédéric Joliot, Orsay, France (F.F.)  
Revised manuscript accepted for publication July 1, 2016.

Héloïse Bergeret-Cassagne thanks the Association Francophone de Chirurgie Endocrinienne (AFCE) for its financial support.

Address correspondence to Frédérique Frouin, PhD, Laboratoire IMIV, Service Hospitalier Frédéric Joliot, 4 Place du Général Leclerc, 91406 Orsay Cedex, France.

E-mail [frederique.frouin@inserm.fr](mailto:frederique.frouin@inserm.fr)

### Abbreviations

CT, computed tomography; MRI, magnetic resonance imaging; US, ultrasound; 2D, two-dimensional

doi:10.7863/ultra.16.05014

Vocal fold motion was analyzed during free breathing using two-dimensional dynamic ultrasound imaging. Two cadavers were first analyzed to define easily identifiable landmarks. Motion of the laryngeal tract was then analyzed in an axial plane. Left and right arytenoids and thyroid cartilage were defined on images corresponding to abduction and adduction of the laryngeal tract. Associated area measurements were established for 50 healthy subjects. All area indices were significantly larger during abduction than adduction. Symmetry of motion was established by comparing each hemi-larynx, and mobility fractions were defined. Normal values of laryngeal motion during free breathing were thus established.

**Key Words**—larynx; ultrasonography; vocal fold motion

The anatomy of the respiratory and phonation tract has been described in detail using computed tomography (CT)<sup>1-3</sup> imaging and magnetic resonance imaging (MRI).<sup>4</sup> However, these imaging modalities require dedicated rooms and cannot be performed at patient's bedside. Some teams have explored the relevance of two-dimensional (2D) ultrasound (US) imaging in the anatomical description of the laryngeal tract.<sup>5-10</sup> For diagnostic or monitoring purposes, US represents an interesting alternative to CT and MRI because of its lower cost, availability, noninvasiveness, innocuousness, and high-temporal resolution.<sup>3</sup> Furthermore, the high temporal resolution makes possible the dynamic analysis of this region during free breathing. However, image quality issues and the 2D imaging inherent to standard US equipment make the exploration of the laryngeal region still a challenging task. Some teams have depicted the US structure and anatomy of false and true vocal folds in small cohorts.<sup>5,6,8</sup> Klem has shown that the arytenoids were easily identifiable in women in more than 90% of cases.<sup>7</sup> In a larger cohort, Wang et al reported that vocal fold motion using US could be assessed in 87% of patients, and that it was less observable in male subjects and in older patients.<sup>10</sup> Recently, US has been proposed in surgery research to assess vocal fold motion during breathing at rest and detect recurrent nerve paralysis after thyroid surgery.<sup>10-18</sup> It was proposed to estimate the symmetry of the laryngeal tract in abduction and adduction, and diagnosis of recurrent nerve paralysis was based on the visual impression of vocal fold immobility. Most of these

studies reported visual criteria to assess the vocal fold motion. Current debates deal with the choice of appropriate landmarks (true vocal folds, false vocal folds, or arytenoids<sup>15</sup>); the choice of the acquisition plane (axial or lateral view<sup>18</sup>); the choice of observation condition (free breathing, phonation, or Valsalva maneuver<sup>17</sup>); and the development of the method in multiple institutions using various US scanners.<sup>13</sup>

Our study focuses on the definition of quantitative indices in the axial view during free breathing on control subjects. The axial view was selected to define symmetry parameters, and free breathing was chosen because it was the most convenient for subjects. First, we aimed to describe the normal laryngeal tract using 2D US on anatomical subjects to identify and study the echogenicity of the different structures. Second, these structures were defined on healthy subjects during free breathing using dynamic US. Finally, indices were defined to characterize

the physiological motion of the laryngeal tract. This study on healthy subjects was necessary to define the range of measures in neurologically competent larynxes during free breathing.

## Materials and Methods

### Subjects

#### *Ex Vivo US Exploration*

Two cadavers (one female and one male subjects) were first studied to identify precisely the anatomical structures of interest. Needles were used to spot each structure of interest. Thus, the US characteristics of the true vocal folds, false vocal folds, and arytenoids were assessed (Figures 1–3). This first step, comparing ex vivo anatomical structures with US findings, was an essential prerequisite before setting the optimal landmarks,

**Figure 1.** Ex vivo identification of the vocal fold and corresponding ultrasound acquisition. **A.** Insertion of a needle inside the vocal fold. **B.** Positioning of the linear ultrasound probe. **C.** Ultrasound B-mode image, arrows showing the vocal fold (VF) and the needle.

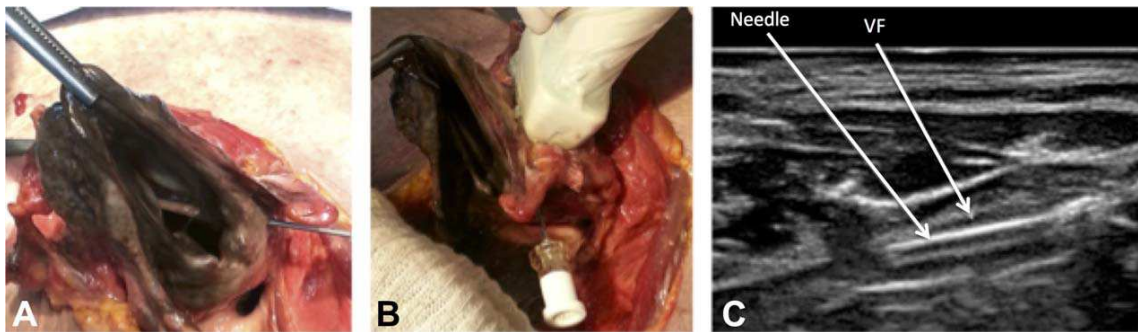
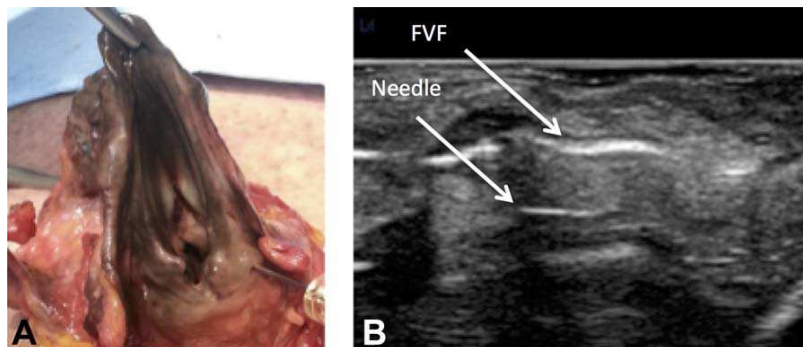


**Figure 2.** Ex vivo identification of the false vocal fold and corresponding ultrasound acquisition. The linear ultrasound probe was placed facing the false vocal fold. **A.** The false vocal fold was spotted with a clamp. **B.** Ultrasound B-mode image: the false vocal fold (FVF) appears hyperechoic.



to generate reproducible and reliable measures on healthy subjects.

*In Vivo Study*

The project was approved by our local ethics committee. Fifty-five subjects were included over the course of 10 months (November 2012 to September 2013) in a tertiary referral center. All subjects gave their informed consent to participate. They were adults with no cervical surgical past, and no ear, nose, or throat diseases. They were referred for thyroid exploration, and the examination proved to be normal. The gender proportion (9 men, 46 women) was defined to mimic the population undergoing thyroid surgery in this center. The mean age and body mass index of the population were 37 years (ranging from 20–58) and 23.5 kg/m<sup>2</sup> (ranging from 18.4–31.5).

*In Vivo US Acquisitions*

All examinations were performed by the same practitioner, using a SonixTouch US machine (UltraSonix, Richmond, BC, Canada) with a linear probe. The subjects were lying on their back with their neck slightly

extended (Figure 4). After applying US gel, the probe was placed over the laryngeal prominence of the thyroid cartilage, to include the arytenoids in the axial view. The images were acquired in B-mode, during normal breathing at rest. Typical values for acquisition were frequency 10 MHz, depth of field of view 4 cm, mechanical index 0.6, gain 45%, dynamic range 85 dB. A loop of 10 s (30 images per second) was then recorded, to include at least one complete respiratory cycle.

*Geometrical Measurements*

Dedicated software was designed to analyze the recorded loops off-line. First, the expert who acquired the loops selected two images corresponding to physiological abduction and adduction in the same breath. Her choice was guided by the relative position of arytenoids and false vocal folds in the field of view. She then placed landmarks on these images (Figure 5) according to the findings of the ex vivo study (Figures 1–3 and “Results” section). The first landmark corresponded to the anterior insertion (A) of the two vocal folds on the thyroid cartilage, and the two others landmarks to the center of the right (R) and left (L) arytenoid cartilages. The

**Figure 3.** Ex vivo identification of the arytenoid cartilage and corresponding ultrasound acquisition. **A.** The needle was placed inside the left arytenoid cartilage. **B.** Ultrasound B-mode image: the left arytenoid cartilage was a hyperechoic round structure.

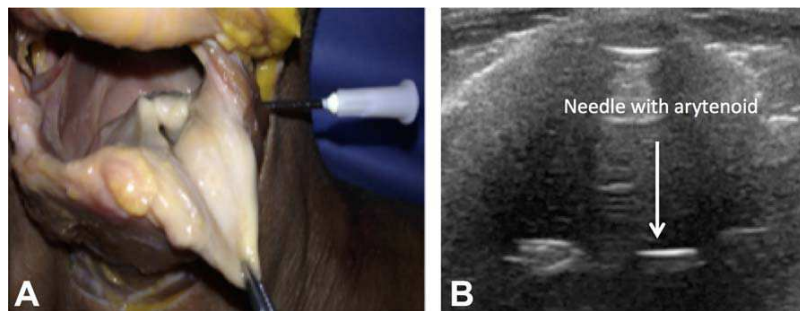


**Figure 4.** In vivo ultrasound acquisition. The linear probe was placed transversely over the middle portion of the thyroid cartilage.



median line crossed the line connecting R and L at a point called M (Figure 5). More than 30 measures were generated including lengths, angles, and surface areas associated with these four points (A, R, L, and M). Because of high correlations existing among these measurements, indices based on surface areas were finally retained. To check the symmetry between the two hemilarynxes, which is a prerequisite in normal subjects, the left and right surfaces  $S_l$  and  $S_r$  were defined according to the areas of the two triangles LAM and RAM. In the case of symmetry, the

difference between the left and right surfaces ( $S_r - S_l$ ) should be close to zero. A dimensionless standardized surface difference,  $\Delta S_s = (S_r - S_l) / S$ ,  $S$  being the surface of the ALR triangle, was computed to make intersubject comparisons easier. Finally, global, left, and right mobility fraction indices,  $MF$ ,  $MF_l$  and  $MF_r$  (Equations (1–3)), were defined to describe motion between the abduction image (superscript “ab”) and the adduction image (superscript “ad”) as follows:

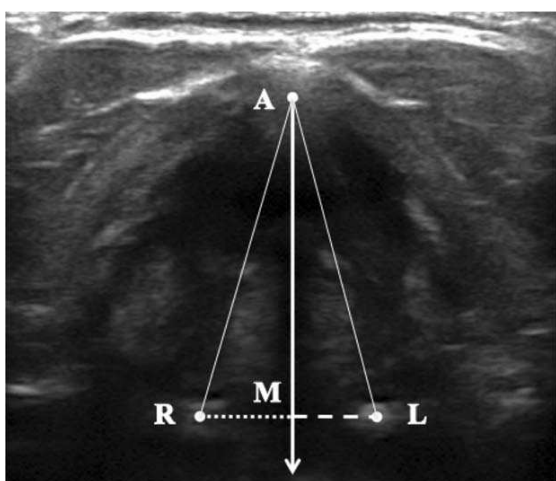
$$MF = (S^{ab} - S^{ad}) / S^{ab}, \quad (1)$$

$$MF_l = (S_l^{ab} - S_l^{ad}) / S_l^{ab}, \quad (2)$$

and

$$MF_r = (S_r^{ab} - S_r^{ad}) / S_r^{ab}. \quad (3)$$

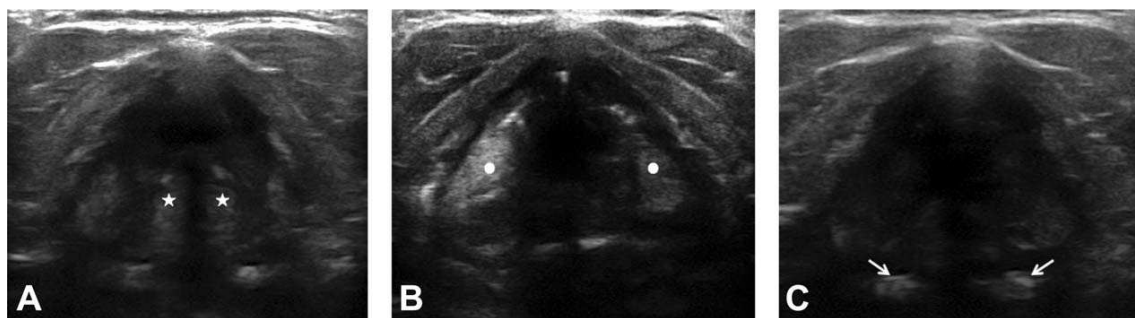
**Figure 5.** Positioning of the three landmarks on the ultrasound B-mode image (axial view). The operator placed A as the most anterior and medial point of the thyroid cartilage, R as the center of the right arytenoid cartilage, and L as the center of the left arytenoid cartilage. The point M was defined from these three landmarks as the intersection of the median line (issued from A) with the line connecting the two arytenoid cartilages.



#### Reproducibility and Statistical Analyses

The means and standard deviations of the measures were computed. For each side, the measures during abduction and adduction were compared using Student’s t-test for paired samples. Similarly, the symmetry of the healthy larynx was evaluated by comparing right and left measures. To assess the performance of our approach as an everyday tool for clinicians, the results obtained by the expert operator were compared with the results obtained by a trained operator who was not a clinician, but who was taught how to place the landmarks during a single session of 1 h. For each measure, a regression analysis was conducted, providing the slope (a) and the intercept (b) of the linear and the correlation coefficient (r). Statistical analyses were performed using JMP software (SAS institute, Cary, NC).

**Figure 6.** Axial view of the laryngeal tract in a healthy subject: **A**, vocal folds (stars) are isoechoic; **B**, false vocal folds (dots) are hyperechoic; **C**, arytenoid cartilages (arrows) are hyperechoic. Right and left sides are symmetric.



## Results

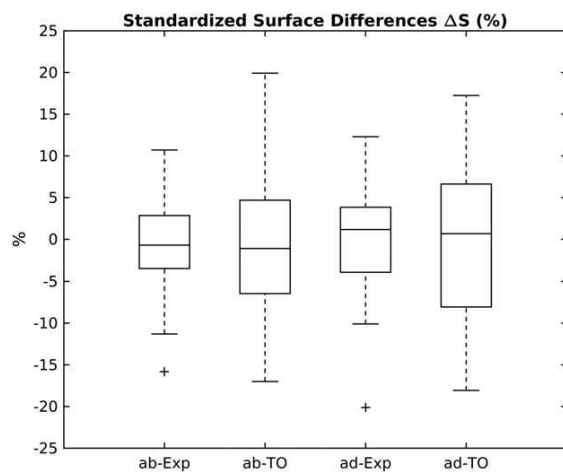
### Ex Vivo US Study

In the male subject, because of the ossified thyroid cartilage, we had to drill the lateral part of the cartilage to obtain interpretable US images, without acoustic shadowing. The echogenicity of the structures (visually assessed) was similar for the two subjects. True vocal folds were isoechoic or hypoechoic (Figure 1). False vocal folds were thicker and more echoic (Figure 2). Arytenoid cartilages were hyperechoic and easy to identify, thanks to their round aspect and posterior location (Figure 3).

### Dynamic Laryngeal Description in Healthy Subjects

Five male subjects were excluded, because their thyroid cartilage generated an acoustic shadow in the US image. In the remaining population, the echogenicity of the structures of interest was similar to the ex vivo study (Figure 6). The true vocal folds, thin and hidden by the false vocal folds, were difficult to follow during breathing, partly because of their out-of-plane motion. It was easier to track the false vocal folds. However, because they are indirect markers of vocal fold motion, the analysis focused on the arytenoid cartilages that make the vocal folds move. The arytenoids were easily identified in all subjects, thanks to their hyperechoic character, surrounded by hypoechoic structures and air.

**Figure 7.** Box plots showing the distribution of standardized surface differences (n = 50), estimated in abduction (ab-) and adduction (ad-) by the expert (Exp) and the trained operator (TO).



### Measures of Arytenoid Cartilage Motion and Symmetry of Larynx

The parameters related to surface areas (Figure 7 and Table 1) and to mobility fractions (Figure 8) were obtained for all subjects. All of the surface areas in abduction were significantly larger than areas in adduction. Furthermore, no significant difference was found between the left and right sides, and standardized surface differences were close to zero (Figure 7). This proves the symmetry of the larynx in static images and during motion (comparing MF<sub>l</sub> with MF<sub>r</sub>).

### Reproducibility of Quantitative Measures

For the area parameters, the reproducibility analyses (Table 2) provided excellent correlations ( $r \geq 0.90$ ), with slopes close to 1 and intercepts close to 0. The

**Table 1.** Measures Related to Surface Areas in Healthy Subjects (N = 50) and Statistical Comparison Between Adduction and Abduction Measures

Surface Area Parameters	Abduction (mean ± standard deviation)	Adduction (mean ± standard deviation)
S (mm <sup>2</sup> )	126 ± 32.1	94.4 ± 31.8 <sup>a</sup>
S <sub>r</sub> (mm <sup>2</sup> )	63.6 ± 17.1	47.5 ± 17.0 <sup>a</sup>
S <sub>l</sub> (mm <sup>2</sup> )	62.1 ± 15.6	46.9 ± 15.4 <sup>a</sup>
ΔS <sub>s</sub> (%)	0.87 ± 5.22	0.18 ± 6.27 <sup>b</sup>

<sup>a</sup>Significant differences with P values less than 10<sup>-4</sup>.

<sup>b</sup>No significant differences.

**Figure 8.** Box plots showing the distribution of global (G-), left (L-), and right (R-) mobility fractions (n = 50), estimated by the expert (Exp) and the trained operator (TO).

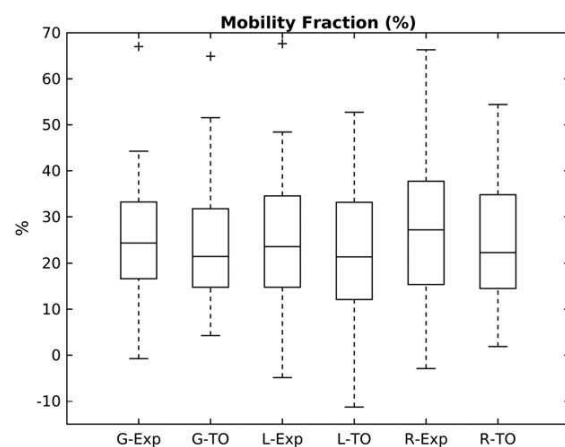


**Table 2.** Reproducibility of Quantitative Measures in Healthy Subjects (N = 50) Between the Expert and Trained Operator

Motion Parameters	Linear Regression Coefficients		
	r	a	b
$S_r^{ab}$ (mm <sup>2</sup> )	0.93	1.05	-0.76
$S_l^{ab}$ (mm <sup>2</sup> )	0.91	1.00	1.75
$S_r^{ad}$ (mm <sup>2</sup> )	0.91	0.91	6.68
$S_l^{ad}$ (mm <sup>2</sup> )	0.91	0.89	7.00
$\Delta S_s^{ab}$ (%)	0.57	0.93	0.02
$\Delta S_s^{ad}$ (%)	0.51	0.80	3.28
MF <sub>r</sub> (%)	0.75	0.70	5.58
MF <sub>l</sub> (%)	0.74	0.80	3.28

Note: r, correlation coefficient; a, slope; b, intercept defined from the linear regression.

correlation was high for the mobility fractions. The correlation was medium for the standardized differences between the left and the right larynx surface areas. This effect was partly the result of  $\Delta S_s$  values that are positive or negative, close to zero, and do not show any specific information, in case of normal symmetric motion. Figures 7 and 8 show the boxplot distribution of standardized difference areas and mobility fractions, for the expert and the trained operator. No statistical differences were found between the mean values estimated by the two operators. However, the values of  $\Delta S_s$  estimated by the expert are less dispersed than the corresponding values estimated by the trained operator (Figure 7), and the values of mobility fractions estimated by the expert tend to be slightly higher than the ones estimated by the trained operator (Figure 8).

## Discussion

Anatomical descriptions of the larynx using US has already been reported.<sup>5,7-9,19</sup> However, these studies did not specifically focus on the laryngeal tract physiological motion. The present ex vivo and in vivo studies allowed a systematic US description of laryngeal structures. The dynamic in vivo study was designed to follow abduction and adduction during free breathing in 50 healthy subjects. As previously stated,<sup>10</sup> the echogenicity of the tissues was similar in men and women, when the ossification of the thyroid cartilage was not an obstacle. The true vocal folds were hypoechoic and difficult to identify and follow with 2D dynamic US during breathing. Choosing the arytenoids as markers of the true vocal fold motion appeared to be more accurate than using the false vocal folds. Indeed, true vocal fold lateral

motion is driven by the arytenoids, themselves moved by the intrinsic laryngeal muscles.

The acquisition was based on one axial view, which is easy to reproduce for competent people in the neck anatomy. In the population that was finally included (all female and 44% of male subjects), arytenoids could be easily identified, independently of the age and the body mass index.

The chosen landmarks were easy to localize even for a trained operator, as shown by the reproducibility analysis. Because surface areas were the basic components of the derived indices, their high reproducibility was primordial to check. The hemilaryngeal right and left measures in healthy subjects were statistically similar and were relevant to distinguish abduction from adduction. On 50 healthy subjects, the mean values of the standardized surface differences  $\Delta S_s$  were less than 1%. Their standard deviations being approximately 5%, values of  $\Delta S_s$  greater than 10% could suggest a dissymmetrical motion. On the same population, mean values of mobility fractions were 25% and standard deviations between 12 and 14%. There are multiple reasons for the larger variability of mobility fractions, including various amplitude breaths during the acquisition. Furthermore, some uncertainties in the localization of the landmarks could imply, in some rare cases, low values of mobility fractions. For that reason, an automated tracking of the landmarks should be investigated. Finally, if the maximal value of mobility fraction cannot be defined, it can be foreseen that patients with paralysis would have reduced values for either left or right mobility fractions.

The procedure that is proposed depends on the operator's expertise. First, the acquisition should be performed in the axial plane, to study the motion symmetry correctly. Our first experiment has shown that a specialist of the larynx can learn how to acquire US data quite easily and quickly. Then the images corresponding to extreme locations of the arytenoids during abduction and adduction have to be selected. Some quality criteria, including the stability of the position of the probe and the signal homogeneity, were checked for this selection. Indeed, this choice was crucial for defining mobility fractions correctly. The last step of the procedure consists of selecting the three points of interest on previously selected images. For this step, an interoperator study was performed that shows a very good agreement between the expert and the trained operator. Not surprisingly, the results obtained by the expert show slightly

less variations, especially for the  $\Delta S_x$  parameters. In addition, some image processing procedures have been proposed to automate the selection of images and to track the landmarks from the abduction image to the adduction image.<sup>20</sup> At the present time, these automated methods cannot replace the expert, because of the complexity of these images. However, they could guide an inexperienced operator.<sup>21</sup>

As already reported by several teams,<sup>10,22</sup> the main limitation of this US approach is the ossification of the thyroid cartilage that occurs in approximately 50% of the male population. In the context of thyroid surgery, which is performed in 80% of women versus 20% of men,<sup>23</sup> the limitation observed on the male population would concern only a small number of cases. Furthermore, as recently proposed by Woo et al, lateral acquisitions and dedicated quantification could be developed for these subjects.<sup>18</sup>

Our next step is to determine the effect of the proposed quantitative analysis in the diagnosis and follow-up of impaired laryngeal motion in a population operated for thyroid pathology. The present study will help in defining thresholds to infer motion abnormality: High values of the standardized surface differences should suggest an impaired motion between the left and right vocal folds, whereas low values of left or right mobility fractions are expected in the case of left or right palsy.

In conclusion, dynamic US in axial view provides a relevant description of laryngeal anatomical structures and arytenoid motion. Because of their high echogenicity, arytenoids are proposed as surrogate markers to characterize vocal fold motion. By selecting three clearly defined landmarks, reproducible and objective measures of abduction and adduction during breathing at rest were obtained. These measures were reported for a database of 50 control subjects, and clearly showed that the movement of the arytenoids can be quantified and that it is symmetrical. The next step will be to evaluate these indices for recurrent nerve paralysis diagnosis.

## References

1. Yumoto E, Sanuki T, Hyodo M. Three-dimensional endoscopic images of vocal fold paralysis by computed tomography. *Arch Otolaryngol Head Neck Surg* 1999; 125:883–890.
2. Tom K, Titze IR, Hoffman EA, Story BH. Three-dimensional vocal tract imaging and formant structure: varying vocal register, pitch, and loudness. *J Acoust Soc Am* 2001; 109:742–747.
3. Prasad A, Yu E, Wong DT, Karkhanis R, Gullane P, Chan VW. Comparison of sonography and computed tomography as imaging tools for assessment of airway structures. *J Ultrasound Med* 2011; 30: 965–972.
4. Flaherty RF, Seltzer S, Campbell T, Weisskoff RM, Gilbert RJ. Dynamic magnetic resonance imaging of vocal cord closure during deglutition. *Gastroenterology* 1995; 109:843–849.
5. Raghavendra BN, Horii SC, Reede DL, Rumancik WM, Persky M, Bergeron RT. Sonographic anatomy of the larynx, with particular reference to the vocal cords. *J Ultrasound Med* 1987; 6: 225–230.
6. Dedejusz M, Adamczewski Z, Brzeziński J, Lewinski A. Real-time, high-resolution ultrasonography of the vocal folds—a prospective pilot study in patients before and after thyroidectomy. *Langenbecks Arch Surg* 2010; 395:859–864.
7. Klem C. Head and neck anatomy and ultrasound correlation. *Otolaryngol Clin North Am* 2010; 43:1161–1169.
8. Singh M, Chin KJ, Chan VWS, Wong DT, Prasad GA, Yu E. Use of sonography for airway assessment an observational study. *J Ultrasound Med* 2010; 29:79–85.
9. Kristensen MS. Ultrasonography in the management of the airway. *Acta Anaesthesiologica Scandinavica* 2011; 55:1155–1173.
10. Wang CP, Chen TC, Yang TL, et al. Transcutaneous ultrasound for evaluation of vocal fold movement in patients with thyroid disease. *Eur J Radiol* 2012; 81:e288–291.
11. Bergeret-Cassagne H. Echographic description of the laryngeal tract: study of vocal fold motion after thyroid surgery. Assessment of a new diagnostic tool for detecting recurrent nerve paralysis. Master's thesis, University Paris-Est, Champs-sur-Mame, France; 2013.
12. Wong KP, Lang BH, Ng SH, Cheung CY, Chan CT, Lo CY. A prospective, assessor-blind evaluation of surgeon-performed transcutaneous laryngeal ultrasonography in vocal cord examination before and after thyroidectomy. *Surgery* 2013; 154:1158–1164.
13. Carneiro-Pla D, Miller BS, Wilhelm SM, et al. Feasibility of surgeon-performed transcutaneous vocal cord ultrasonography in identifying vocal cord mobility: a multi-institutional experience. *Surgery* 2014; 156:1597–1602.
14. Wong KP, Lang BH, Ng SH, Cheung CY, Chan CT, Chan MY. Is vocal cord asymmetry seen on transcutaneous laryngeal ultrasonography a significant predictor of voice quality changes after thyroidectomy? *World J Surg* 2014; 38:607–613.
15. Wong KP, Woo JW, Youn YK, Chow FC, Lee KE, Lang BH. The importance of sonographic landmarks by transcutaneous laryngeal ultrasonography in post-thyroidectomy vocal cord assessment. *Surgery* 2014; 156:1590–1596.
16. Wong KP, Lang BH, Chang YK, Wong KC, Chow FC. Assessing the validity of transcutaneous laryngeal ultrasonography (TLUSG) after thyroidectomy: what factors matter? *Ann Surg Oncol* 2015; 22:1774–1780.